First Principles Based Reaction Kinetics for Decomposition of Hot Dense Liquid TNT from ReaxFF Multiscale Reactive Dynamics Simulations

Naomi Rom[1*], Barak Hirshberg[1], Yehuda Zeiri[3,4], David Furman[1], Sergey V. Zybin[2], William A. Goddard III[2], and Ronnie Kosloff[1]

[1]Fritz Haber Research Center for Molecular Dynamics, Hebrew University, Jerusalem 91904, Israel
[2]Materials and Process Simulation Center, 139-74, California Institute of Technology, Pasadena, California 91125, USA
[3]Bio-medical Engineering, Ben Gurion University, Beer-Sheva 84105, Israel
[4]Division of Chemistry, NRCN, P.O. Box 9001 Beer-Sheva 84190, Israel

* nomir@fh.huji.ac.il (972-2-658-5485)

Supporting Information

1. AMORPHOUS LIQUID TNT PREPARATION AND THERMAL DECOMPOSITION

The liquid TNT cell prepared using the scheme outlined in Section 2.2 (denoted *liquid 1*) reminisces some of the long range order that exists in the TNT crystal (see FIG. 1 below and FIG. 3 in the paper), while its density is very close to the measured one at 400K.

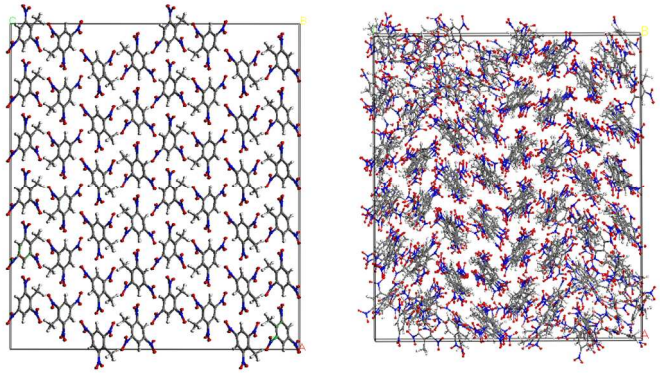

FIG. 1: The energy-minimized TNT crystal supercell (left) and the liquid simulation cell at 1atm, 400K (right) shown in FIG. 2 in the paper are presented here from a different direction.

In order to study the effect of liquid preparation scheme on its structure and thermal decomposition, a different approach was used to construct liquid TNT cell at 400K and 1 atm (denoted *liquid 2*):

- 36 TNT molecules were *randomly* placed in a unit cell (a,b,c = 23.64, 19.13, 20.79 Å) and the cell energy was minimized. Thereafter, the unit cell was 2x2x2 expanded, obtaining a 288 TNT molecules supercell with dimensions similar to those of *liquid 1* (a, b, c = 47.28, 38.26, 41.57 Å, density 1.444 gr/cm^3). The supercell energy was minimized using LAMMPS with ReaxFF LG-corrected potentials[6]. The amorphous crystal cell obtained is plotted below in FIG. 2 and FIG. 3.
- The crystal was heated to 400K, beyond TNT's measured melting point, then thermalized for 20 ps.
- Atmospheric pressure was applied at 400K via 30 ps long NPT simulation. The average density obtained was 1.35 gr/cm^3, ~6% *lower* than the measured one.
- Finally, the cell was thermalized at 400K for 2 ps and relaxed using NVE for additional 2 ps. See *liquid 2* cell in FIG. 4 and FIG. 5.

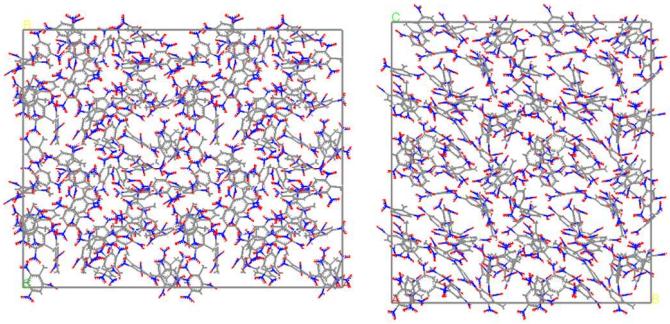

FIG. 2: Two facets of energy-minimized amorphous TNT crystal supercell.

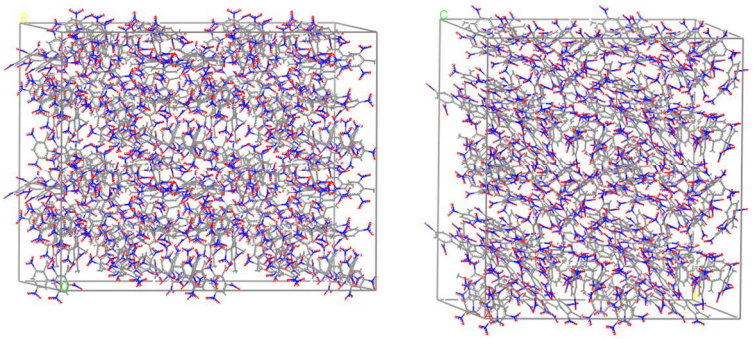

FIG. 3: As FIG. 2, from a different perspective.

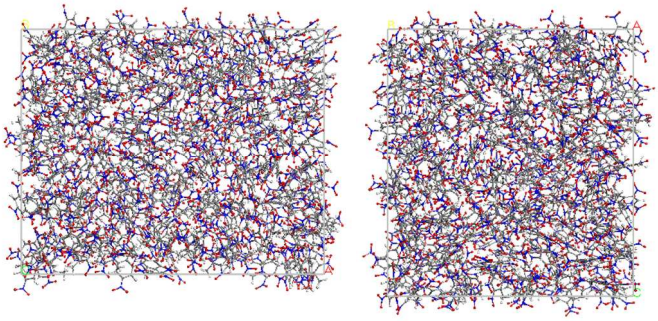

FIG. 4: Two facets of amorphous TNT liquid cell (*liquid 2*) at 1 atm and 400K, at the end of NVE relaxation.

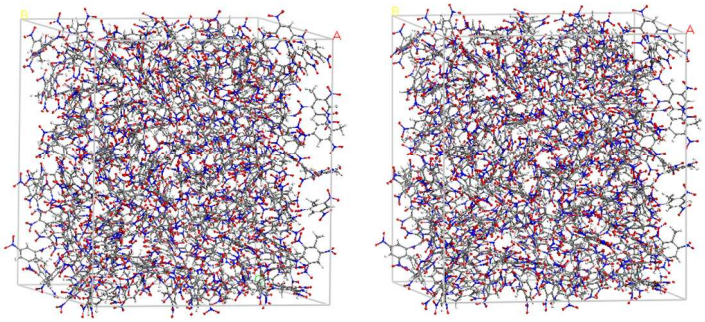

FIG. 5: As FIG. 4, from a different perspective.

The heat-up simulations for TNT *liquid 2* were performed using the method described in Section 2.4, at 2250K, 2700K and 3500K. A comparison between the decay of the TNT molecules in liquid cells *1* and *2* is shown in FIG. 6 at these temperatures. The decay of *liquid 2* is slightly slower compared to *liquid 1* decay. This is expected due to the lower density, hence larger inter-molecular distances, in *liquid 2* which decelerates inter-molecular reactions and decomposition.

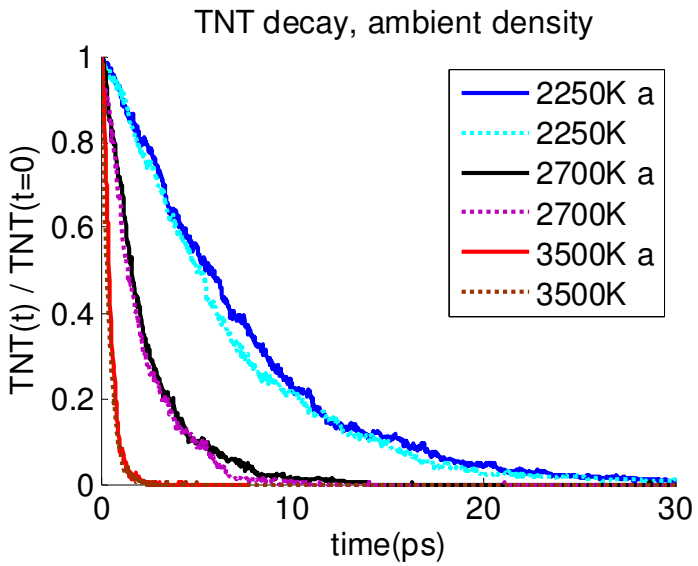

FIG. 6: TNT molecules decay for *liquid 2* (denoted in the legend by *a - for amorphous*) and *liquid 1* vs. simulation time, at various temperatures.

Thermal rate constants were calculated for the endothermic (k_1) and exothermic (k_2) stages of *liquid 2* decomposition. In FIG. 7 Arrhenius plots of *liquid 2* rate constants are compared to those of *liquid 1*. The activation energy and pre-factor logarithm, $\ln(A_0\ [sec^{-1}])$, for k_1 are 35.2 kcal/mole and 33.4, and for k_2 23.5 kcal/mole and 29.1, respectively. These values resemble those of the uncompressed *liquid 1* (see Table 2 and Table 3 in the paper).

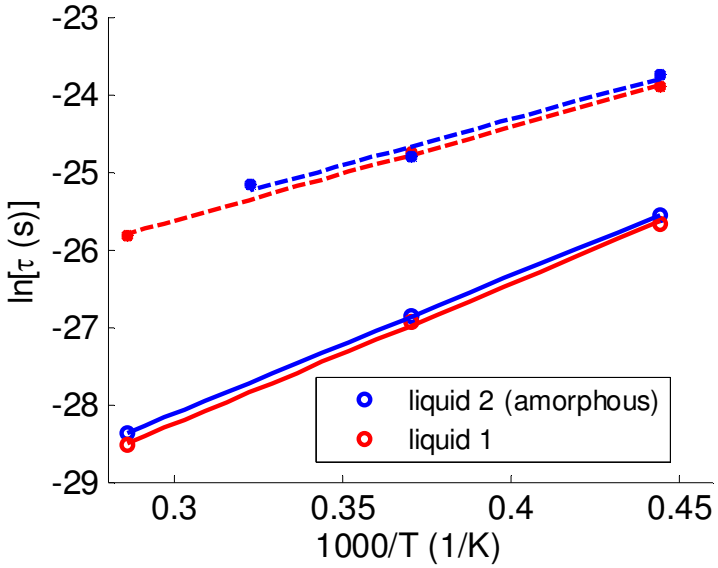

FIG. 7: Arrhenius plots for TNT *liquid 1* and *liquid 2* thermal decomposition. The endothermic stage rate constant (k_1) is plotted with full lines, whereas the exothermic stage rate constant (k_2) is plotted with dashed lines. Per liquid cell, the initial density is the density at 400K and 1 atm. Temperature range is 2250K-3500K.

Some dominant initial fragments created in the decomposition of liquid TNT at 2250K are plotted in FIG. 8 for *liquid 2* and *liquid 1*. It is seen that there are small differences in the decomposition characteristics of the two TNT liquid cells. In FIG. 9 the main initial fragments, NO and NO_2, are presented for heat-up simulations at various temperatures. It is seen that initially, in the uni- or bi-molecular reactions stage, the creation of the fragments is similar for

both liquid cells (density effect is small), whereas the reactions are slower in the later stages in the lower density *liquid 2*. This effect decreases with increasing temperature.

.

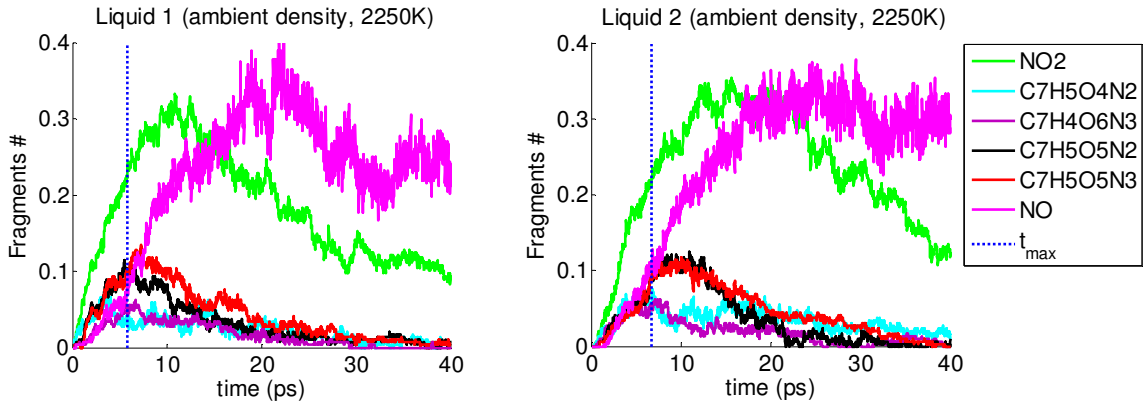

FIG. 8: Selected initial fragments created in the thermal decomposition of *liquid 1* (left) and *liquid 2* (right) in heat-up simulation at 2250K (ambient density).

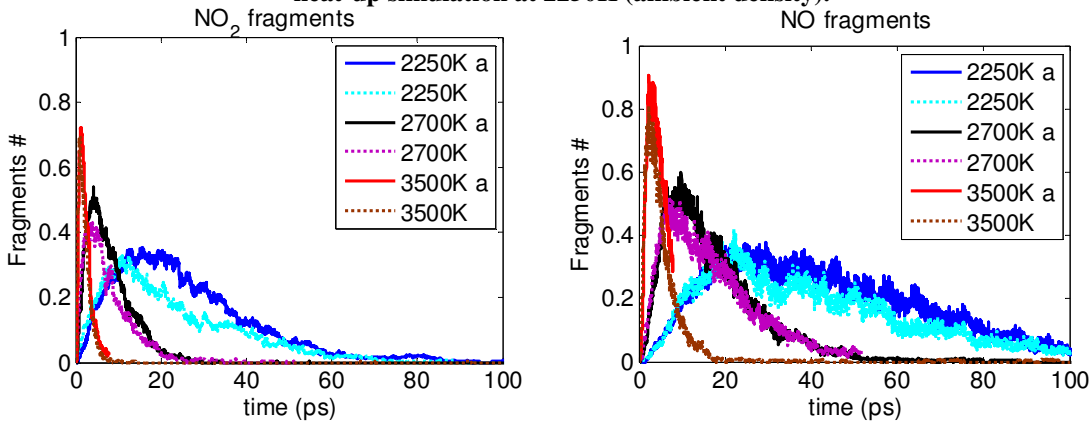

FIG. 9: NO (right) and NO_2 (left) fragments created in the thermal decomposition simulations of *liquid 2* (full lines, denoted in the legend by *a* - for *amorphous*) and *liquid 1* (dotted lines) at various temperatures.

Finally, in FIG. 10 some small gaseous final products created in the thermal decomposition of the two liquid cells (*1* and *2*) at 2700K are plotted. H_2O and N_2 formation is delayed in *liquid 2*, whereas the carbon containing gases (CO and CO_2) are created faster. This can be understood, again, based on the higher proximity of the TNT molecules (and fragments) in denser *liquid 1*. Thus, in *liquid 1* decomposition, both small gaseous fragments that do not contain carbon atoms (e.g. H_2O and N_2) and larger, carbon-rich clusters are created faster, while small carbon-containing fragments creation is delayed.

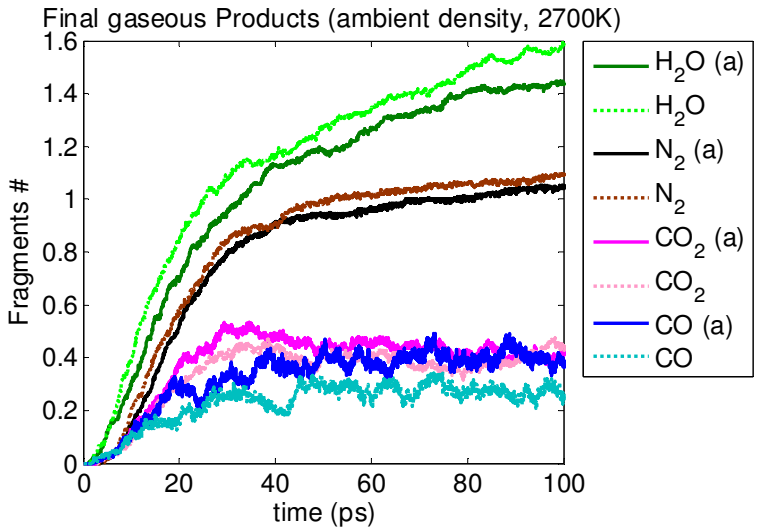

FIG. 10: Final gaseous products creation at 2700K for *liquid 1* (dotted lines) and *liquid 2* (full lines, denoted "a").

2. PRESSURE AND POTENTIAL ENERGY EVOLUTION

The time evolution of the total pressure and potential energy as a function of density (see Table 1 in the paper) is presented in FIG. 11 and FIG. 12. Generally, the pressure increases with temperature and compression. In all cases, the pressure profiles reach an asymptotic limit. At low compressions (0 and 15%) the pressure increases, while it decreases at 30% compression. This density dependence can be explained by the formation of large clusters at high compression that causes reduction of the gaseous products and pressure (see Section 4 in the paper).

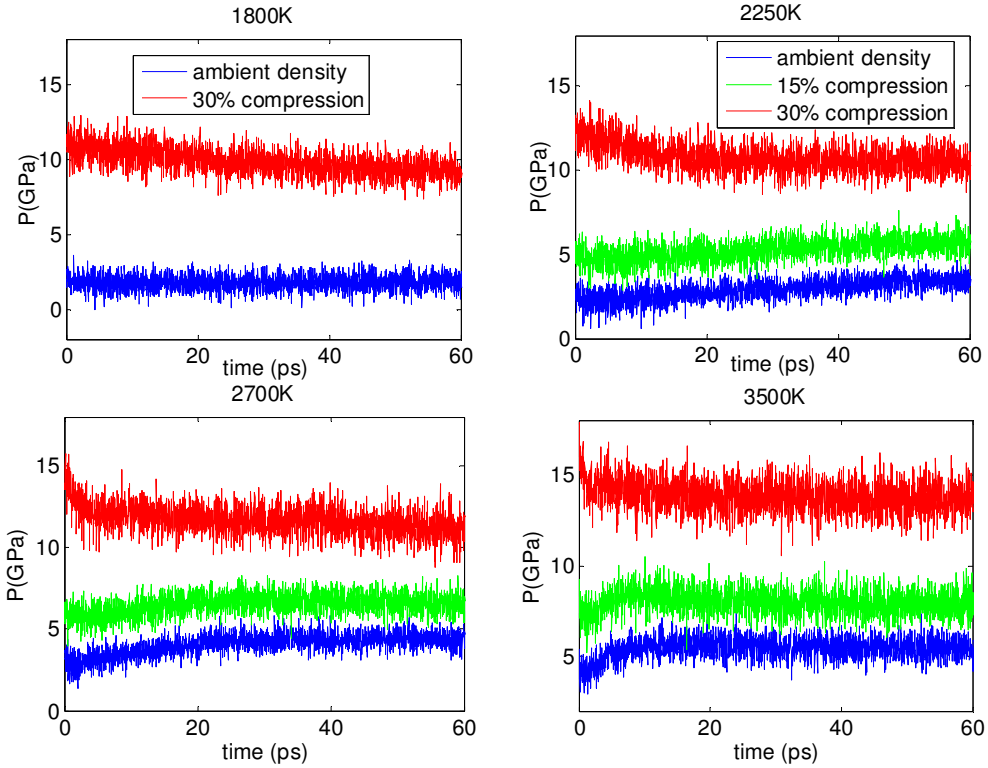

FIG. 11: Pressure vs. simulation time for various densities (ambient density – blue, 15% compression – green, 30% compression – red), plotted separately per constant temperature simulation (1800-3500K).

The variation of the system PE during the decomposition process is presented in FIG. 12. Although the simulations are carried out at a constant temperature (and kinetic energy), energy is consumed and released during the simulation due to chemical bond rupture and formation. The calculated PE profile can be divided into two parts: A short increasing part, which is related to the endothermic initial decomposition step, and a decreasing part, related to the exothermic reactions that take place following the initial part.

The influence of compression on the PE profile is demonstrated in FIG. 12. For all temperatures examined, the asymptotic potential energy reduces as the compression increases. This means that the final products are more stable at high compressions. This result can be explained by a more effective and complete decomposition of liquid TNT at these high pressures. A second observation is that the energy released (calculated as the difference between the asymptotic value of PE and the barrier energy) is larger at high compressions. In addition, at each temperature shown in FIG. 12, the PE reaches its maximal and asymptotic values faster as compression increases. This is in agreement with the liquid TNT decay rate increase as compression rises (see FIG. 4 in the paper).

The temperature dependence of the PE is presented in FIG. 13 for 30% compression. It is clear that the completion of the liquid TNT decomposition is faster at higher temperatures. The amount of energy released in the exothermic part of the PE is similar at all temperatures studied, with only ~2% variation between the lowest and highest temperatures.

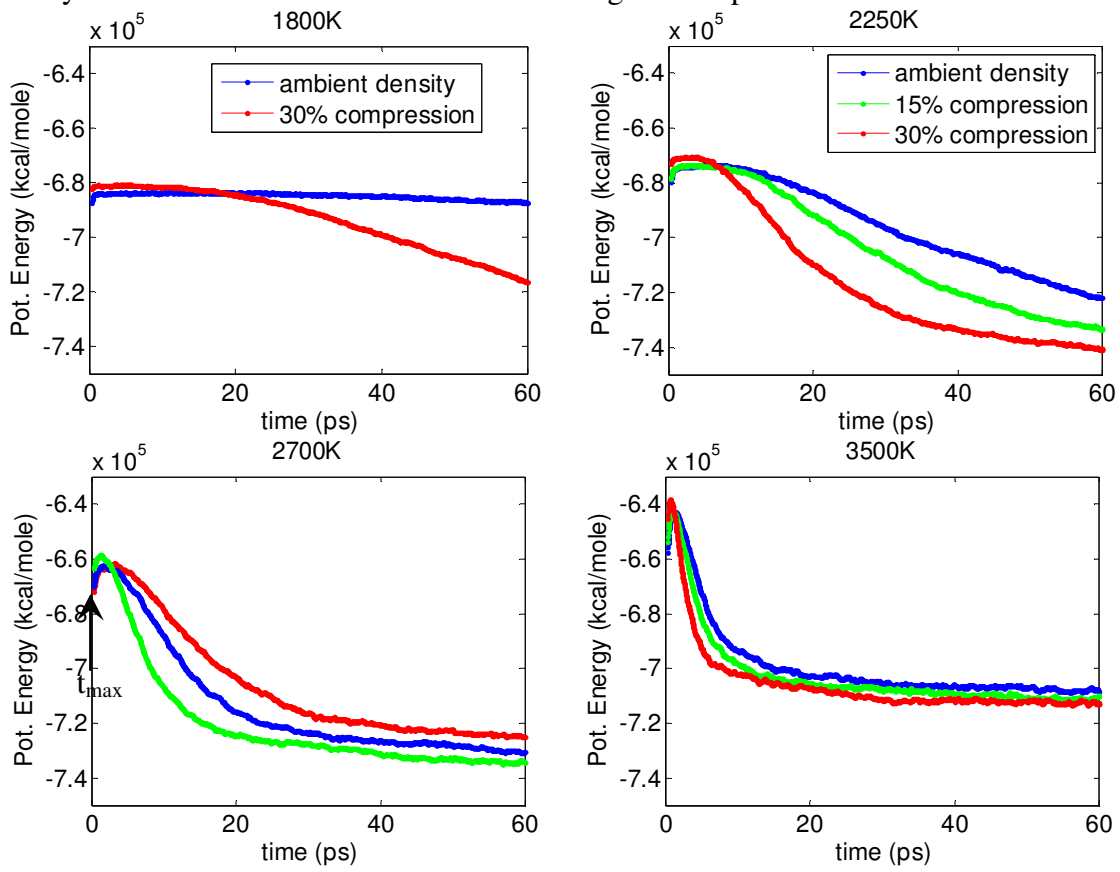

FIG. 12: Potential energy vs. simulation time for various densities, plotted separately per constant temperature simulation (1800-3500K). t_{max} is the PE maximum, separating between the endothermic and exothermic stages in the decomposition reaction of liquid TNT. Energy units are kcal/mole, where "mole" here refers to a mole of simulation cells.

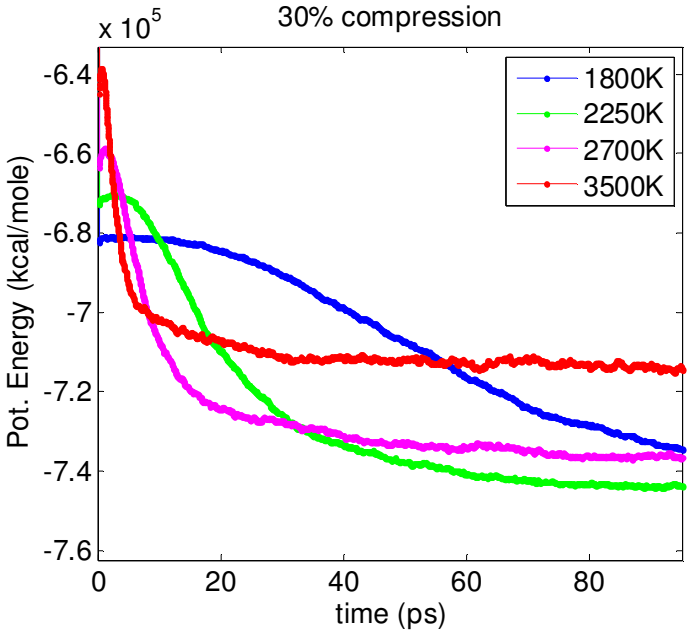

FIG. 13: Potential energy vs. simulation time for 30% compressed liquid TNT, at various temperatures.

3. BOND ORDER CUTOFF VALUES

In order to determine whether a bond exists between every two atom pairs in the ReaxFF MD simulation, at each time step the calculated bond orders are compared with the relevant bond order cutoff values supplied within the fragments analysis code. The cutoff values used in the fragment analysis presented in this manuscript are given in Table 1 below.

Table 1: Atom pairs (atom#1 and atom#2) bond order cutoff values employed in the fragments analysis.

Atom #1	Atom #2	Bond order cut off
C	N	0.3
C	C	0.55
C	O	0.65
C	H	0.4
O	O	0.65
N	O	0.40
O	H	0.40
H	H	0.55
H	N	0.55
N	N	0.55

4. FRAGMENTS ANALYSIS: INITIAL AND INTERMEDIATE REACTIONS

Below, additional results for the initial and intermediate fragments formed during liquid TNT decomposition are shown, at ambient density and 30% compression. In FIG. 14, additional initial fragments created at 1800K are plotted (complementary to FIG. 8 in the paper), and in FIG. 15 - FIG. 17 fragments created at 2250K and 2700K are shown. A blow up of FIG. 15 (ambient

density, 2250K - see FIG. 16) focuses on the initial decomposition reactions obtained: (1) Unimolecular NO_2 release; (2) TNT dimer decomposition, producing $C_7H_5O_5N_2$, $C_7H_5O_5N_3$ and NO_2. The vertical line (dashed, blue) represents t_{max}, the time when exothermic reactions initiate.

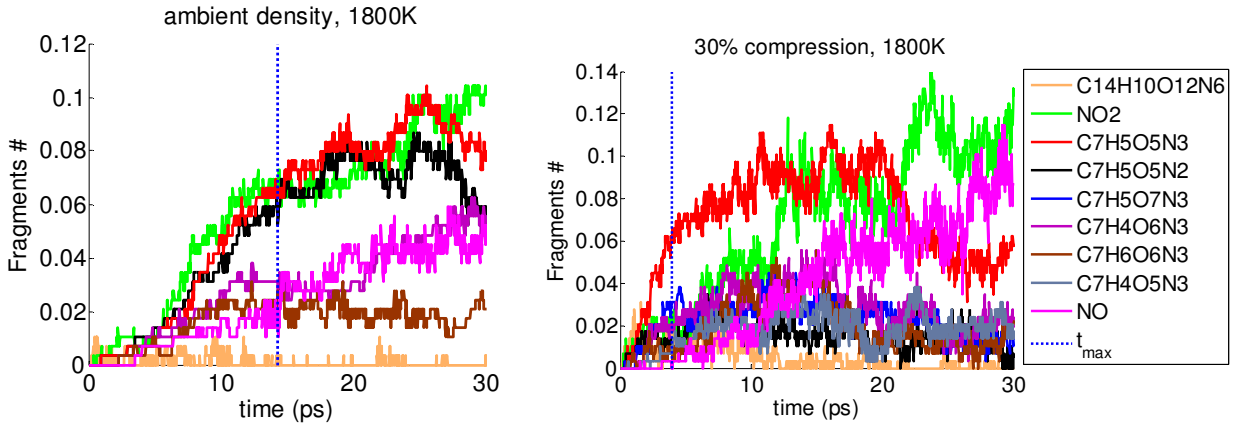

FIG. 14: Additional fragments at 1800K liquid TNT decomposition for ambient density (left) and 30% compression (right).

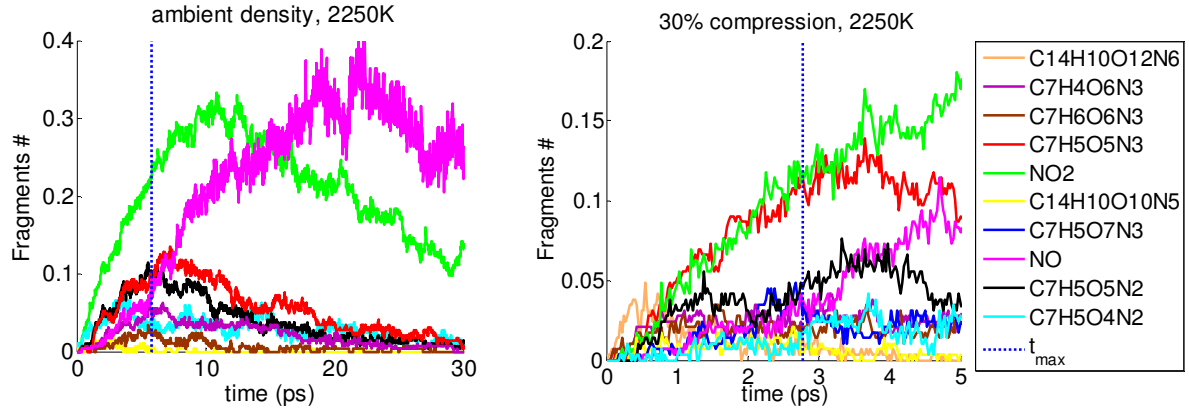

FIG. 15: A comparison between the initial fragments created at ambient density (left) and 30% compression (right) at 2250K.

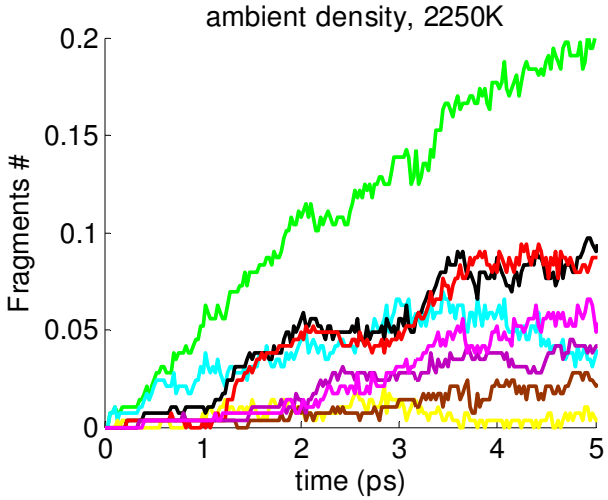

FIG. 16: Blow up of FIG. 15 for ambient density liquid TNT at 2250K, focusing on the initial decomposition reactions.

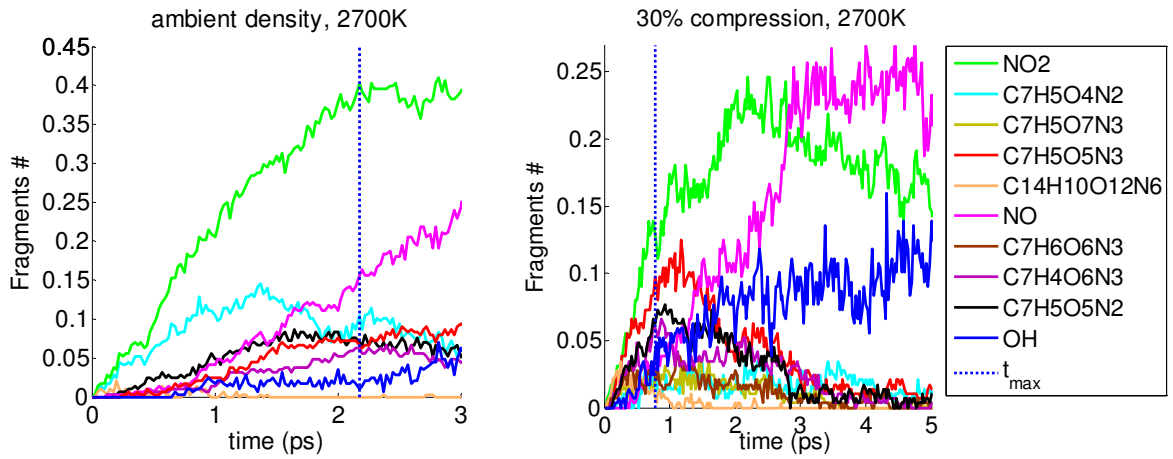

FIG. 17: A comparison between the initial fragments created at ambient density (left) and 30% compression (right) at 2700K.

5. REAXFF PARAMETERS

Reactive MD-force field nitramines (RDX/HMX/TATB/PETN): Strachan, A.; et al. Phys. Rev. Lett. 2003, 91, 098301

```
 39       ! Number of general parameters
50.0000 !Overcoordination parameter
9.4514 !Overcoordination parameter
30.0000 !Valency angle conjugation parameter
216.4305 !Triple bond stabilisation parameter
12.4838 !Triple bond stabilisation parameter
0.0000 !C2-correction
1.0701 !Undercoordination parameter
7.5000 !Triple bond stabilisation parameter
11.9083 !Undercoordination parameter
13.3822 !Undercoordination parameter
10.4637 !Triple bond stabilization energy
0.0000 !Lower Taper-radius
10.0000 !Upper Taper-radius
2.8793 !Not used
33.8667 !Valency undercoordination
3.5895 !Valency angle/lone pair parameter
1.0563 !Valency angle
2.0384 !Valency angle parameter
6.1431 !Not used
6.9290 !Double bond/angle parameter
0.0283 !Double bond/angle parameter: overcoord
0.0570 !Double bond/angle parameter: overcoord
-2.4837 !Not used
5.8374 !Torsion/BO parameter
10.0000 !Torsion overcoordination
1.8820 !Torsion overcoordination
-1.2327 !Conjugation 0 (not used)
2.1861 !Conjugation
1.5591 !vdWaals shielding
0.0100 !Cutoff for bond order (*100)
```

5.2216 !Valency angle conjugation parameter
3.4021 !Overcoordination parameter
38.5241 !Overcoordination parameter
2.1533 !Valency/lone pair parameter
0.5000 !Not used
20.0000 !Not used
5.0000 !Molecular energy (not used)
2.0000 !Version number
6.5560 !Valency angle conjugation parameter
4 ! Nr of atoms; cov.r; valency;a.m;Rvdw;Evdw;gammaEEM;cov.r2;#
alfa;gammavdW;valency;Eunder;Eover;chiEEM;etaEEM;n.u.
cov r3;Elp;Heat inc.;n.u.;n.u.;n.u.;n.u.
ov/un;val1;n.u.;val3,vval4
C 1.3742 4.0000 12.0000 1.9684 0.1723 0.8712 1.2385 4.0000
9.4606 2.1346 4.0000 31.0823 79.5548 5.7254 6.9235 0.0000
1.2104 0.0000 183.7012 5.7419 33.3951 11.9957 0.8563 0.0000
-2.8983 2.5000 1.0564 4.0000 2.9663 0.0000 0.0000 0.0000
0.0001 1.9255
H 0.6867 1.0000 1.0080 1.3525 0.0616 0.8910 -0.1000 1.0000
9.3858 5.0013 1.0000 0.0000 121.1250 3.8446 10.0839 1.0000
-0.1000 0.0000 58.4228 3.8461 3.2540 1.0000 1.0698 0.0000
-15.7683 2.1504 1.0338 1.0000 2.8793 0.0000 0.0000 0.0000
0.0001 1.4430
O 1.3142 2.0000 15.9990 1.9741 0.0880 0.8712 1.1139 6.0000
10.2186 7.7719 4.0000 29.5271 116.0768 8.5000 7.1412 2.0000
0.9909 14.9473 69.2812 9.1371 1.6258 0.1863 0.9745 0.0000
-3.5965 2.5000 1.0493 4.0000 2.9225 0.0000 0.0000 0.0000
623.8417 1.7500
N 1.2450 3.0000 14.0000 1.9951 0.1088 1.0512 1.1911 5.0000
9.9303 7.8431 4.0000 32.4758 100.0000 6.7768 6.8035 2.0000
1.0636 0.1045 128.0119 2.1604 2.9464 2.5181 0.9745 0.0000
-4.0959 2.0047 1.0183 4.0000 2.8793 0.0000 0.0000 0.0000
1240.001 1.8300
10 ! Nr of bonds; Edis1;LPpen;n.u.;pbe1;pbo5;13corr;pbo6
pbe2;pbo3;pbo4;Etrip;pbo1;pbo2;ovcorr
1 1 141.9346 113.4487 67.6027 0.1554 -0.3045 1.0000 30.4515 0.4283
0.0801 -0.2113 8.5395 1.0000 -0.0933 6.6967 1.0000 0.0000
1 2 163.6889 0.0000 0.0000 -0.4525 0.0000 1.0000 6.0000 0.5921
12.1053 1.0000 0.0000 1.0000 -0.0097 8.6351 0.0000 0.0000
2 2 169.8421 0.0000 0.0000 -0.3591 0.0000 1.0000 6.0000 0.7503
9.3119 1.0000 0.0000 1.0000 -0.0169 5.9406 0.0000 0.0000
1 3 164.0476 117.4881 72.1261 -0.6031 -0.1795 1.0000 14.9755 0.5413
1.2626 -0.3063 7.0000 1.0000 -0.1588 4.5000 0.0000 0.0000
3 3 110.4748 155.6441 40.0000 0.1150 -0.1054 1.0000 28.5221 0.2000
0.9590 -0.2635 8.5715 1.0000 -0.1007 6.8548 1.0000 0.0000
1 4 130.7147 175.2276 97.2523 -0.0368 -0.4942 1.0000 26.7545 0.5133
0.3296 -0.3653 7.0000 1.0000 -0.1171 5.1025 1.0000 0.0000
3 4 85.4950 114.0081 70.1453 0.5778 -0.1070 1.0000 16.6611 0.2339
0.3474 -0.1948 8.3762 1.0000 -0.1089 5.8148 1.0000 0.0000
4 4 157.7518 67.1322 160.9732 -0.5869 -0.1824 1.0000 12.0000 0.7136
0.8204 -0.1657 10.6490 1.0000 -0.0967 4.5976 1.0000 0.0000
2 3 224.3076 0.0000 0.0000 -0.6280 0.0000 1.0000 6.0000 1.0000
5.0050 1.0000 0.0000 1.0000 -0.0512 5.1982 0.0000 0.0000
2 4 212.1772 0.0000 0.0000 -0.3585 0.0000 1.0000 6.0000 0.3316
10.4316 1.0000 0.0000 1.0000 -0.0658 6.4545 0.0000 0.0000
6 ! Nr of off-diagonal terms; Ediss;Ro;gamma;rsigma;rpi;rpi2

```
1  2   0.0464   1.8296  10.1311   1.0029  -1.0000  -1.0000
2  3   0.0375   1.7275  10.8037   0.8813  -1.0000  -1.0000
2  4   0.0509   1.7672  10.4261   0.9990  -1.0000  -1.0000
1  3   0.1036   1.8869   9.5668   1.3590   1.1099   1.1534
1  4   0.1971   1.7356  10.0734   1.2754   1.2113   1.1172
3  4   0.0535   1.6709  10.8180   1.2968   1.1416   1.0167
42    ! Nr of angles;at1;at2;at3;Thetao,o;ka;kb;pv1;pv2
1  1  1  74.0317  32.2712   0.9501   0.0000   0.1780  10.5736   1.0400
1  1  2  70.6558  14.3658   5.3224   0.0000   0.0058   0.0000   1.0400
2  1  2  76.7339  14.4217   3.3631   0.0000   0.0127   0.0000   1.0400
1  2  2   0.0000   0.0000   6.0000   0.0000   0.0000   0.0000   1.0400
1  2  1   0.0000   3.4110   7.7350   0.0000   0.0000   0.0000   1.0400
2  2  2   0.0000  27.9213   5.8635   0.0000   0.0000   0.0000   1.0400
1  1  3  65.3104   6.3897   7.5000   0.0000   0.2000  10.0000   1.8525
3  1  3  71.9855  28.5708   6.4252   0.0000   0.2000   0.0000   1.8525
1  1  4  65.8892  45.0000   1.6598   0.0000   0.2000  10.0000   1.8525
3  1  4  73.1057  25.8227   4.2145   0.0000   0.2000   0.0000   1.8525
4  1  4  65.8759  40.9838   2.4369   0.0000   0.2000   0.0000   1.8525
2  1  3  56.3039  17.3681   5.3095   0.0000   0.9110   0.0000   1.0400
2  1  4  71.5505  11.1820   3.7129   0.0000   0.9110   0.0000   1.0400
1  2  4   0.0000   0.0019   6.3000   0.0000   0.0000   0.0000   1.0400
1  3  1  72.3642  37.8942   1.1566   0.0000   0.7472   0.0000   1.2639
1  3  3  90.0000  45.0000   0.5719   0.0000   0.7472   0.0000   1.2639
1  3  4  70.4313  14.4055   7.1593   0.0000   0.7472   0.0000   1.2639
3  3  3  83.8833  23.3345   2.3433 -10.0000   0.7472   0.0000   1.2639
3  3  4  84.0407  45.0000   1.0695   0.0000   0.7472   0.0000   1.2639
4  3  4  73.9966  24.4410   5.2760   0.0000   0.7472   0.0000   1.2639
1  3  2  89.1394  37.0874   0.3849   0.0000   3.0000   0.0000   1.2618
2  3  3  80.7068   5.0854   5.7151   0.0000   3.0000   0.0000   1.2618
2  3  4  76.0238  45.0000   0.8637   0.0000   3.0000   0.0000   1.2618
2  3  2  82.3474  13.5165   3.4896   0.0000   0.3596   0.0000   1.3307
1  4  1  68.4330  19.3525   2.1625   0.0000   1.7325   0.0000   1.0440
1  4  3  86.2893  37.5587   1.2660   0.0000   1.7325   0.0000   1.0440
1  4  4  74.2404  12.0547   7.5000   0.0000   1.7325   0.0000   1.0440
3  4  3  78.5566  43.8492   1.3351 -26.1471   1.7325  40.0000   1.0440
3  4  4  77.4239  33.7297   1.7944  -0.9193   1.7325   0.0000   1.0440
4  4  4  64.9107  17.5558   7.5000   0.0000   1.7325   0.0000   1.0440
1  4  2  90.0000  32.0540   0.7195   0.0000   0.5355   0.0000   2.5279
2  4  3  84.1185  45.0000   1.3826   0.0000   0.5355   0.0000   2.5279
2  4  4  78.7133  24.6250   3.8202   0.0000   0.5355   0.0000   2.5279
2  4  2  56.3036  14.1532   3.3914   0.0000   0.2000   0.0000   2.1689
1  2  3   0.0000   0.0019   6.0000   0.0000   0.0000   0.0000   1.0400
1  2  4   0.0000   0.0019   6.0000   0.0000   0.0000   0.0000   1.0400
1  2  5   0.0000   0.0019   6.0000   0.0000   0.0000   0.0000   1.0400
3  2  3   0.0000   0.0019   6.0000   0.0000   0.0000   0.0000   1.0400
3  2  4   0.0000   0.0019   6.0000   0.0000   0.0000   0.0000   1.0400
4  2  4   0.0000   0.0019   6.0000   0.0000   0.0000   0.0000   1.0400
2  2  3   0.0000   0.0019   6.0000   0.0000   0.0000   0.0000   1.0400
2  2  4   0.0000   0.0019   6.0000   0.0000   0.0000   0.0000   1.0400
17    ! Nr of torsions;at1;at2;at3;at4;;V1;V2;V3;V2(BO);vconj;n.u;n
1  1  1  1   0.0000  48.4194   0.3163  -8.6506  -1.7255   0.0000   0.0000
1  1  1  2   0.0000  63.3484   0.2210  -8.8401  -1.8081   0.0000   0.0000
2  1  1  2   0.0000  45.2741   0.4171  -6.9800  -1.2359   0.0000   0.0000
0  1  2  0   0.0000   0.0000   0.0000   0.0000   0.0000   0.0000   0.0000
0  2  2  0   0.0000   0.0000   0.0000   0.0000   0.0000   0.0000   0.0000
0  1  3  0  -0.0002  85.8794   0.3236  -3.8134  -2.0000   0.0000   0.0000
```

```
0  2  3  0   0.0000   0.1000   0.0200  -2.5415   0.0000   0.0000   0.0000
0  3  3  0  -0.9667 116.4743   0.0002  -4.9422   0.0000   0.0000   0.0000
0  1  4  0  -0.0069 150.0000   0.4891  -7.4921  -2.0000   0.0000   0.0000
0  2  4  0   0.0000   0.1000   0.0200  -2.5415   0.0000   0.0000   0.0000
0  3  4  0   1.6745  56.6301  -0.0008  -4.5064  -2.0000   0.0000   0.0000
0  4  4  0   1.1253  75.3447   0.0080  -9.0000  -2.0000   0.0000   0.0000
0  1  1  0   0.0930  18.5962   0.0002  -9.0000  -1.0000   0.0000   0.0000
4  1  4  4  -2.0000  20.8732  -1.5000  -9.0000  -2.0000   0.0000   0.0000
1  1  3  3  -0.0002  21.5452   0.1727  -9.0000  -2.0000   0.0000   0.0000
1  3  3  1   0.0002  79.3777  -1.5000  -5.2139  -2.0000   0.0000   0.0000
3  1  3  3  -1.3476  22.4932   1.5000  -9.0000  -2.0000   0.0000   0.0000
4    ! Nr of hydrogen bonds;at1;at2;at3;Rhb;Dehb;vhb1
3  2  3   2.0000  -5.0000   3.0000   3.0000
3  2  4   1.7753  -5.0000   3.0000   3.0000
4  2  3   1.3884  -5.0000   3.0000   3.0000
4  2  4   1.6953  -4.0695   3.0000   3.0000
```